Isotope Ratios of H, C, and O in CO2 and H2O of the Martian Atmosphere
Chris R. Webster *et al.*
Science **341**, 260 (2013);
DOI: 10.1126/science.1237961

$$\mathrm{MR}(B) \equiv \frac{R(B) - R(0)}{R(0)} = \frac{I(0) - I(B)}{I(B)} \quad (3)$$

where $R(B)$ is the resistance at magnetic field B and $R(0)$ the resistance at zero field. We have derived $\mathrm{MR}_{\max}(V)$ from the I-Vs for different channel lengths at zero magnetic field and maximum magnetic field, $B_{\max}$, according to $\mathrm{MR}_{\max}(V) = [I(V,0) - I(V,B_{\max})]/I(V,B_{\max})$, (Fig. 4C). The MR increases rapidly with decreasing voltage, reaching a maximum value of more than 2000% for 60-nm wire length when approaching 0 V. Because the current levels are below the noise limit close to 0 V, we have not been able to determine $\mathrm{MR}_{\max}$ here.

The MR values in our molecular wires compare favorably with values reported for other systems under similar conditions. The highest room-temperature TMR value reported to date is 600% for an epitaxial CoFeB/MgO/CoFeB magnetic tunnel junction (24). Collosal magnetoresistance (CMR) manganites exhibit very large low-temperature MR at several tesla (25); however, room-temperature, low-field MR values are a few tens of percents (26, 27). For nanocomposites containing magnetic nanoparticles, MR values similar to those in CMR experiments have been demonstrated under comparable experimental conditions (28). A large room-temperature MR effect of a few tens of percents was also reported for a graphene nanoribbon field-effect transistor (29).

We ascribe our very large MR values to the unique 1D character of our system. Indeed, nonstructured DXP thin films show much lower MR values (Fig. 4D). When a ~40-nm DXP film is contacted with a PtSi CP-AFM tip in the same setup, we measure a maximum MC of around −20%. With a Pt wire of 250-μm diameter instead of the PtSi tip, the maximum MC is reduced to about −5%. These results strongly suggest that confinement of the current path is crucial for explaining our results, in line with recent numerical studies (9). Explanations based on spin-dependent interactions involving excited states (30, 31) can be ruled out, because the MR is also present—and even more pronounced— below the DXP HOMO-LUMO gap (~2 eV). The fact that for DXP the energy required to form doubly negatively charged states is remarkably small [~0.2 eV from cyclic voltammetry measurements (23)] suggests that such states are involved in transport. We therefore propose that the current is carried by electrons and that spin blockade is caused by two electrons residing on neighboring molecules attempting to form a doubly negatively charged molecule in a spin-singlet configuration by hopping of one of the electrons. The energetic disorder generally present in organic systems facilitates formation of doubly charged molecules at favorable locations. Moreover, the presence of a positively charged potassium ion close to a DXP molecule strongly reduces its LUMO level, also facilitating double charging. Simula-

tions show that with these ingredients, MC values close to −100% indeed can be obtained with MC (B) curves having the line shape of Eq. 2 (10). Further analysis should provide more insight into the details of the mechanism behind the effect, but the present experimental results clearly point at spin blockade tuned by a competition between the external magnetic field and the random internal hyperfine field.

References and Notes

1. M. N. Baibich et al., Phys. Rev. Lett. 61, 2472–2475 (1988).
2. G. Binasch, P. Grünberg, F. Saurenbach, W. Zinn, Phys. Rev. B 39, 4828–4830 (1989).
3. M. Jullière, Phys. Lett. 54, 225–226 (1975).
4. J. S. Moodera, L. R. Kinder, T. M. Wong, R. Meservey, Phys. Rev. Lett. 74, 3273–3276 (1995).
5. K. Ono, D. G. Austing, Y. Tokura, S. Tarucha, Science 297, 1313–1317 (2002).
6. R. Hanson, L. P. Kouwenhoven, J. R. Petta, S. Tarucha, L. M. K. Vandersypen, Rev. Mod. Phys. 79, 1455–1455 (2007).
7. T. Francis, Ö. Mermer, G. Veeraraghavan, M. Wohlgenannt, New J. Phys. 6, 185 (2004).
8. W. Wagemans et al., Spin 1, 93–108 (2011).
9. S. P. Kersten, S. Meskers, P. A. Bobbert, Phys. Rev. B 86, 045210 (2012).
10. Materials and methods are available as supplementary materials on Science Online.
11. G. Calzaferri, S. Huber, H. Maas, C. Minkowski, Angew. Chem. Int. Ed. 42, 3732–3758 (2003).
12. P. Bornhauser, G. Calzaferri, J. Phys. Chem. 100, 2035–2044 (1996).
13. P. A. Anderson et al., Dalton Trans. 19, 3122–3128 (2004) and references therein.
14. M. J. Kelly, J. Phys. Condens. Matter 7, 5507–5519 (1995).
15. T. Bein, in Recent Advances and New Horizons in Zeolite Science and Technology, H. Chon, S. I. Woo, S. E. Park, Eds. (Elsevier, Amsterdam, 1996), pp. 295–322.
16. D. J. Cardin, Adv. Mater. 14, 553 (2002).
17. U. Simon, M. E. Franke, in Host-Guest-Systems Based on Nanoporous Crystals, F. Laeri, F. Schüth, U. Simon, M. Wark, Eds. (Wiley, Weinheim, 2003), pp. 364–378.
18. M. Álvaro et al., Chem. Mater. 18, 26–33 (2006).
19. F. J. Jansen, R. A. Schoonheydt, J. Chem. Soc., Faraday Trans. 69, 1338 (1973).
20. Z. K. Tang et al., Science 292, 2462 (2001).
21. A. M. Nardes et al., Org. Electron. 9, 727–734 (2008).
22. H. Bentmann, A. A. Demkov, R. Gregory, S. Zollner, Phys. Rev. B 78, 205302 (2008).
23. S. K. Lee et al., J. Am. Chem. Soc. 121, 3513–3520 (1999).
24. S. Ikeda et al., Appl. Phys. Lett. 93, 082508 (2008).
25. G. Q. Gong et al., Appl. Phys. Lett. 67, 1783 (1995).
26. P. K. Siwach, H. K. Singh, O. N. Srivastava, J. Phys. Condens. Matter 20, 273201 (2008).
27. Y.-T. Zhang, Z.-Y. Chen, C.-C. Wang, Q. Jie, H.-B. Lü, J. Magn. Magn. Mater. 321, 1199–1201 (2009).
28. F. J. Yue et al., J. Phys. D Appl. Phys. 44, 025001 (2011).
29. J. Bai et al., Nat. Nanotechnol. 5, 655–659 (2010).
30. V. N. Prigodin, J. D. Bergeson, D. M. Lincoln, A. J. Epstein, Synth. Met. 156, 757–761 (2006).
31. P. Desai, P. Shakya, T. Kreouzis, W. P. Gillin, Phys. Rev. B 76, 235202 (2007).

Isotope Ratios of H, C, and O in CO2 and H2O of the Martian Atmosphere

Chris R. Webster,[1]* Paul R. Mahaffy,[2] Gregory J. Flesch,[1] Paul B. Niles,[6] John H. Jones,[7] Laurie A. Leshin,[3] Sushil K. Atreya,[4] Jennifer C. Stern,[2] Lance E. Christensen,[1] Tobias Owen,[5] Heather Franz,[2] Robert O. Pepin,[8] Andrew Steele,[9] the MSL Science Team†

Stable isotope ratios of H, C, and O are powerful indicators of a wide variety of planetary geophysical processes, and for Mars they reveal the record of loss of its atmosphere and subsequent interactions with its surface such as carbonate formation. We report in situ measurements of the isotopic ratios of D/H and $^{18}O/^{16}O$ in water and $^{13}C/^{12}C$, $^{18}O/^{16}O$, $^{17}O/^{16}O$, and $^{13}C^{18}O/^{12}C^{16}O$ in carbon dioxide, made in the martian atmosphere at Gale Crater from the Curiosity rover using the Sample Analysis at Mars (SAM)'s tunable laser spectrometer (TLS). Comparison between our measurements in the modern atmosphere and those of martian meteorites such as ALH 84001 implies that the martian reservoirs of CO2 and H2O were largely established ~4 billion years ago, but that atmospheric loss or surface interaction may be still ongoing.

The Sample Analysis at Mars (SAM) suite (1) on the Curiosity rover that landed in August 2012 is conducting a search for

organic compounds and volatiles in rocks and soils and characterizing the chemical and isotopic composition of the modern atmosphere. Atmo-

spheric characterization is one of the exploration goals of the Mars Science Laboratory (MSL) mission (2), and it is accomplished using SAM's tunable laser spectrometer (TLS) and its quadrupole mass spectrometer (QMS). Here we focus on TLS measurements; a companion paper (3) focuses on those from the QMS. Results for nondetection by TLS of atmospheric methane are reported elsewhere (4).

Previous measurements of isotopes of H, N, and noble gases in the martian atmosphere to date (5) have indicated enrichment in the heavier isotopes, consistent with the idea of atmospheric loss to space of the lighter isotopes (6, 7). Although meteoritic analyses of δ^{13}C and δ^{18}O (8) in shergottite, nakhlite, and chassigny (SNC)–class meteorites are made at higher precision than the atmospheric measurements to date, they are challenged to correctly account for possible terrestrial contamination (9). Measurements of CO_2 isotopes at Mars and in particular δ^{13}C values have not been consistent with atmospheric loss (10). Viking (11) measured δ^{13}C and δ^{18}O values of 23 ± 43 per mil (‰) and 7 ± 44‰. Earth-based spectroscopy has suggested depleted values for δ^{13}C of –22 ± 20‰ and δ^{18}O of 18 ± 18‰ (9). The recent Phoenix lander measured δ^{13}C and δ^{18}O values for CO_2 in the martian atmosphere of –2.5 ± 4.3‰ and 31 ± 5.7‰, respectively (12). Although uncertainties in these earlier atmospheric measurements of δ^{13}C and δ^{18}O overlap (Table 1), their δ^{13}C values are in marked contrast to measurements of trapped CO_2 in martian meteorite EETA 79001, generally considered to be closest to the true martian atmosphere and which yielded a δ^{13}C of 36 ± 10‰ (8).

For D/H in water, the difference in ground-state energies of HDO and its parent HHO are large enough to cause large changes in δD in equilibrium and nonequilibrium (kinetic) processes (13, 14), especially where condensation or freezing occurs. For this reason, D/H has become a universally important ratio to identify planetary origin and history (7, 15). The 1988 telescopic observation of D/H values in the martian atmosphere that were ~6 times that of Earth (7) were pivotal in the idea of atmospheric loss to space from a dense, warm, ancient atmosphere. Initial measurements in meteorites (16) gave a wide range of D/H values that may have included terrestrial contributions. A more recent analysis (17) of the ancient meteorite ALH84001 (~4 billion years old) and young meteorite Shergotty (0.17 billion years old) produced δD values of 3000

and 4600, respectively. These results have been interpreted (17) as evidence for a two-stage evolution for Martian water—a significant early loss of water to space [before 3.9 billion years ago (Ga)], followed by only modest loss to space during the past 4 billion years. Until Curiosity landed, there had been no in situ measurements of the water isotopic species HDO and $H_2{}^{18}$O.

Oxygen isotopes in carbonates and sulfates from martian meteorites do not show any enrichment in δ^{18}O and therefore have not been used as indicators of atmospheric escape (18, 19).

It has been suggested that they are buffered by interaction with a larger O reservoir such as the silicates in the crust, or crustal ice deposits (20), although this is complicated by evidence for disequilibrium between the crust and the atmosphere (21). Oxygen isotopes in CO_2 and H_2O are therefore likely indicators of more complex interactions between the large reservoir of O in the hydrosphere, lithosphere, and atmosphere of Mars.

TLS is a two-channel tunable laser spectrometer that uses direct and second harmonic detection of infrared (IR) laser light absorbed after

Table 1. Carbon dioxide isotope ratios ‰ ± 2 SEM (standard error of the mean). *, not measured.

Measurement	δ^{13}C	δ^{18}O	δ^{17}O	$\delta^{13}C^{18}$O
SAM-TLS	46 ± 4	48 ± 5	24 ± 5	109 ± 31
SAM-QMS (3)	45 ± 12	*	*	*
Phoenix lander (12)	−2.5 ± 4.3	31.0 ± 5.7	*	*
Viking Neutral Mass Spectrometer (11)	23 ± 43	7 ± 44	*	*
SNC meteorites (8, 12, 32)	36 ± 10	3.9–5.4 ± 0.1	~0.53* δ^{18}O ~ δ^{13}C+ δ^{18}O
ALH84001 meteoritic carbonate range (30, 31)	27 to 64	−9 to 26	~0.53* δ^{18}O ~ δ^{13}C+ δ^{18}O
ALH84001 meteoritic carbonate mean value (31)	46 ± 8	4.6 ± 1.2	*	*
Earth telescopes (9)	−22 ± 21	18 ± 18	*	*

Fig. 1. Spectral scan regions used by the TLS instrument. Calculated spectra from the HITRAN database (36) for measuring CO_2 (**A** and **B**) and H_2O isotope ratios (**B**). The HDO line intensity has been increased by a factor of 6 to better represent the martian environment.
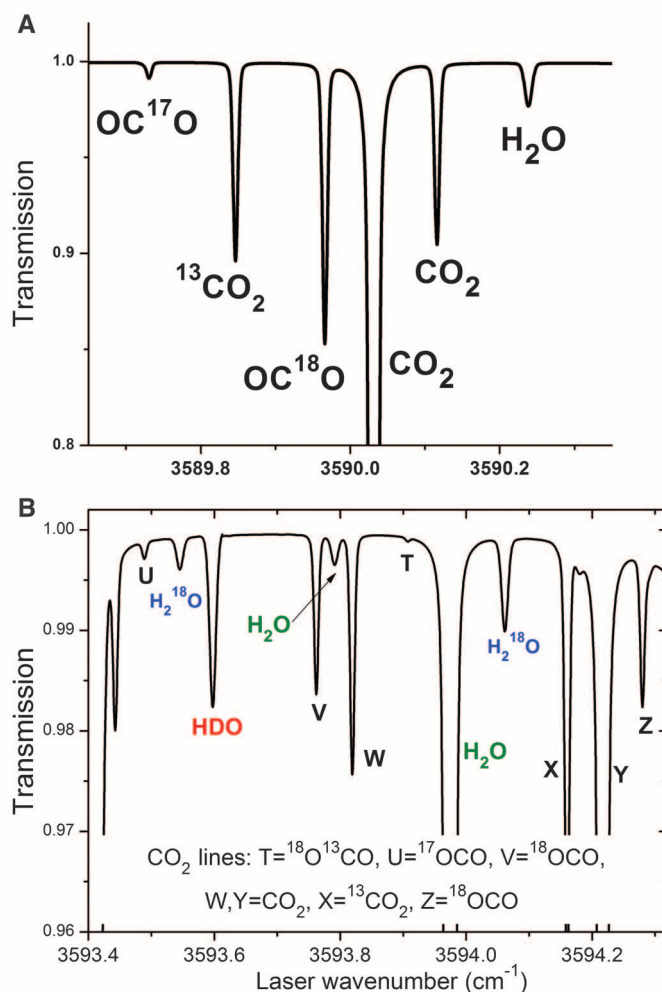
[1]Jet Propulsion Laboratory, California Institute of Technology, Pasadena, CA 91109, USA. [2]NASA Goddard Space Flight Center, Greenbelt, MD 20771, USA. [3]Rensselaer Polytechnic Institute, Troy, NY 12180, USA. [4]University of Michigan, Ann Arbor, MI 48105, USA. [5]University of Hawaii, Honolulu, HI 96822, USA. [6]NASA Johnson Space Center, Houston, TX 77058, USA. [7]University of Arizona, Tucson, AZ 85721, USA. [8]University of Minnesota, Minneapolis, MN 55455, USA. [9]Carnegie Institution of Washington, Washington, DC 20015, USA.

*Corresponding author. E-mail: chris.r.webster@jpl.nasa.gov
†Mars Science Laboratory (MSL) Science Team authors and affiliations are listed in the supplementary materials.

multipassing a sample cell (*1*). One laser source is a near-IR tunable diode laser at 2.78 μm that can scan two spectral regions containing CO_2 and H_2O isotopic lines; the second laser source is an interband cascade laser at 3.27 μm used for methane detection alone (*4*). The near-IR laser makes 43 passes of a 20-cm-long sample (Herriott) cell that is evacuated with a turbomolecular pump for background scans, then filled to 0.7 mbar using volume expansion of Mars air originally at ~7 mbar. TLS scans over individual rovibrational lines in two spectral regions near 2.78 μm; one centered at 3590 cm^{-1} for CO_2 isotopes and a second centered at 3594 cm^{-1} for both CO_2 and H_2O isotopes (Figs. 1 and 2). The lines used in both regions have no significant interferences. In the 3594 cm^{-1} region, the CO_2 and H_2O lines we used interleave across the spectrum without interference, allowing the determination of accurate isotope ratios across widely varying CO_2 and H_2O abundances in both atmospheric and evolved gas experiments. The laser scans every second through the target spectral regions. Each 1-s spectrum is then co-added on board in 2-min periods, and the averaged spectra are then downlinked as raw data during a given run, typically of ~30 min duration. Data reported here were collected from 6 days (martian sols 28, 53, 73, 79, 81, and 106). During data collection, the Herriott cell and other optics are kept at 47° ± 3°C using a ramped heater that also serves to increase the signal-to-noise ratio in spectra by reducing the effect of interference fringes occurring during the 2-min sample period. The measured background amounts (empty cell) of both CO_2 and H_2O are negligible and also reflect an insignificant contribution to the signal from the instrument foreoptics. TLS is calibrated using certified isotopic standards (*22*) that improve the accuracy of isotope ratios over using the more uncertain HITRAN (high-resolution transmission molecular absorption) database spectral parameters.

Our CO_2 isotope ratios (Table 1, table S1, and Fig. 3) are given relative to Vienna Pee Dee belemnite (VPDB) for $\delta^{13}C$ and relative to Vienna standard mean ocean water (VSMOW) for all oxygen isotopes (*13*). The measured value of $\delta^{13}C^{18}O$ agrees within uncertainty to the sum of the individual $\delta^{13}C$ and $\delta^{18}O$ measurements, providing a valuable check-sum on our results. Also, our measured value for $\delta^{17}O$ is half that of $\delta^{18}O$, as predicted from mass-dependent fractionation ($\delta^{17}O = 0.528 \times \delta^{18}O$) and consistent with previous SNC meteorite analysis. The independent SAM QMS result for $\delta^{13}C$ of 45 ± 12‰ (*3*) agrees well with that from TLS at 46 ± 4‰, both values notably disagreeing with the much lower Phoenix lander result (*12*) of −2.5 ± 4.3‰. The sol-by-sol data plotted in Fig. 3 is not over a sufficiently long period to assess possible seasonal variation in $\delta^{13}C$ or $\delta^{18}O$.

Our measured water abundances of up to 1% by volume in our Herriott cell after atmospheric intake exceed those expected (~150 parts per

Fig. 2. Observed versus calculated spectra. A single spectrum (middle section) downloaded from Curiosity (black), showing observed enrichment in $^{13}CO_2$ and ^{18}OCO compared to the calculated HITRAN spectrum (red) based on terrestrial (VPDB and VSMOW) isotope ratios (*36*). Both spectra are normalized in depth to the $^{16}O^{12}C^{16}O$ line near 3590.1 cm^{-1} (Fig. 1). Ringing to the left side of the lines is explained in (*22*).
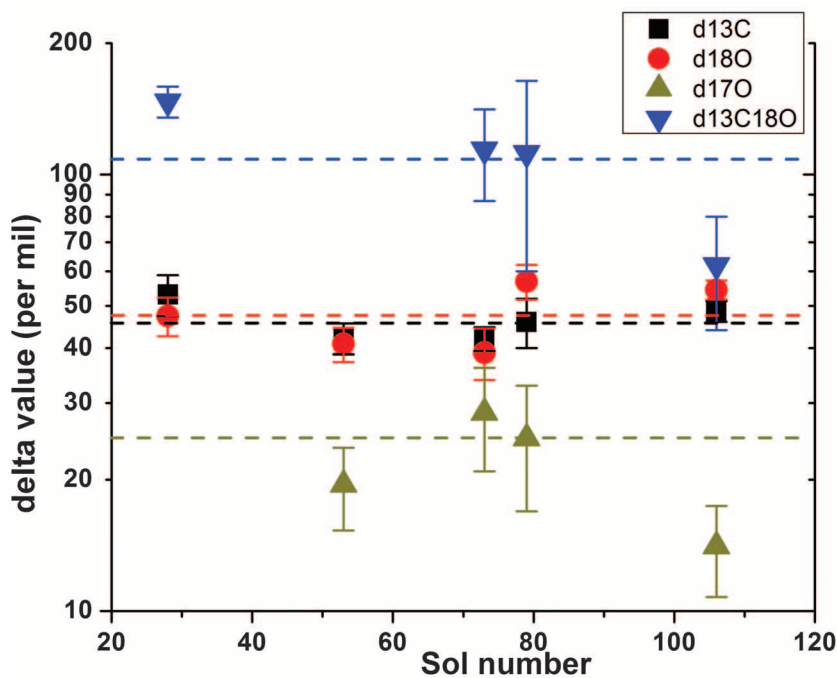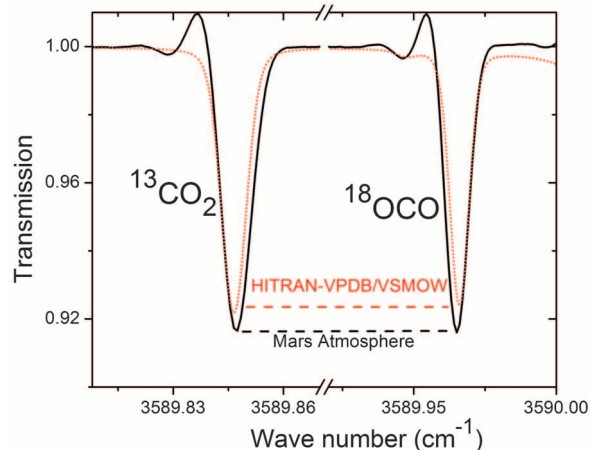
Fig. 3. Sol-by-sol mean values for CO_2 isotope ratios. The mean values for all sols combined (dashed lines) are given in Table 1. See (*22*) for values and uncertainties of the individual sol data plotted.

milion by volume) in martian air, and allowed us to retrieve a value for atmospheric δD, although with high uncertainty. Because our measured highly enriched δD values (Table 2 and table S2) are clearly martian and not terrestrial, we attribute the high water mixing ratios to either high near-surface humidity (natural or from enhanced temperatures in the vicinity of the rover) or to water entrained from frozen or liquid sources on or near the heated inlet valve. Also, in evolved gas experiments from pyrolysis of Rocknest fines (*23*), water was seen coming off at relatively low temperatures that we here identify as representative of the δD and $\delta^{18}O$ values of the martian atmosphere. The TLS measurement of δD agrees well with observations from ground-based telescopes (*24*), but the contribution from expected

seasonal cycling (*25*) is unknown. The enriched atmospheric values contrast with the low primordial D/H values postulated for the martian mantle (*26*) and are higher than those from our Rocknest higher-temperature studies (*23*).

Modeling estimates of escape processes and atmospheric stability during Mars' initial history point to catastrophic loss of atmospheric mass, and suggest that many atmospheric species carrying records of early isotopic evolution did not survive beyond approximately 3.7 to 4 Ga (*27, 28*). Carbonates in the ALH 84001 meteorite derived from an alteration event that occurred at ~3.9 Ga (*29*) preserve our best record of these events. Measurements of ALH 84001 carbonates show enriched isotopic values of $\delta^{13}C$ = +27 to +64‰ (*30, 31*), δD values of ~3000‰ (*16, 17*), and low

Table 2. Water isotope ratios ‰ ± 2 SEM. *, not measured.

Measurement	δD	δ^{18}O
SAM-TLS atmosphere	4950 ± 1,080	*
SAM-TLS evolved water: Rocknest fines 230° to 430°C (23)	5880 ± 60	84 ± 10
Meteoritic crustal reservoirs (26)	~5000	*
Earth telescopes (24)	1700–8900	*
ALH 84001 (17)	3000	*
Shergotty USNM 321-1 (17)	4600	*

δ^{18}O values (32). These values are similar to the composition of the modern martian atmosphere, suggesting that the δ^{13}C, δD, and δ^{18}O of the martian atmosphere were enriched early and have not changed much over ~4 billion years. Our higher values of δD and δ^{18}O measured in the atmosphere suggest that escape processes may have also continued since 4.0 Ga, in accordance with a two-stage evolutionary process (17) described above.

We observe large enrichments of δ^{18}O in atmospheric water vapor and CO_2. The δ^{18}O values of the water vapor are much larger than the δ^{18}O observed in carbonates and sulfates in martian meteorites and suggest that the oxygen in water vapor in the martian atmosphere is not in equilibrium with the crust (33, 34) and could have been enriched in heavy isotopes through atmospheric loss. Another possibility is that the elevated oxygen isotope values in the more abundant martian CO_2 are being transferred to the water vapor through photochemical reactions in the atmosphere. However, δ^{18}O values of CO_2 in Earth's atmosphere are similarly elevated because of low-temperature equilibration between CO_2 and H_2O, and this process could also be operative on Mars (12).

In addition to atmospheric loss, other processes such as volcanic degassing and weathering might act to change the isotopic composition of the atmosphere through time. Estimates for the magnitude of these two contributions over the ~4-billion-year history of Mars vary widely (30, 34, 35), yet could have a strong impact on the isotopic composition of the atmosphere and challenge the status quo model described above.

References and Notes

1. P. R. Mahaffy et al., Space Sci. Rev. **170**, 401–478 (2012).
2. J. P. Grotzinger et al., Space Sci. Rev. **170**, 5–56 (2012).
3. P. R. Mahaffy et al., Science **341**, 263–266 (2013).
4. C. R. Webster, P. R. Mahaffy, S. K. Atreya, G. J. Flesch, K. A. Farley, Lunar Planet. Sci. Conf., abstract 1366 (2013).
5. B. M. Jakosky, R. J. Phillips, Nature **412**, 237–244 (2001).
6. M. B. McElroy, Y. L. Yung, A. O. Nier, Science **194**, 70–72 (1976).
7. T. Owen, J.-P. Maillard, C. de Bergh, B. L. Lutz, Science **240**, 1767–1770 (1988).
8. R. H. Carr, M. M. Grady, I. P. Wright, C. T. Pillinger, Nature **314**, 248–250 (1985).
9. V. A. Krasnopolsky, J. P. Maillard, T. C. Owen, R. A. Toth, M. D. Smith, Icarus **192**, 396–403 (2007).
10. P. B. Niles et al., Space Sci. Rev. **174**, 301–328 (2013).
11. A. O. Nier, M. B. McElroy, Science **194**, 1298–1300 (1976).
12. P. B. Niles, W. V. Boynton, J. H. Hoffman, D. W. Ming, D. Hamara, Science **329**, 1334–1337 (2010).
13. R. E. Criss, Principles of Stable Isotope Composition (Oxford Univ. Press, Oxford, 1999).
14. C. R. Webster, A. J. Heymsfield, Science **302**, 1742–1745 (2003).
15. P. Hartogh et al., Nature **478**, 218–220 (2011).
16. L. A. Leshin, S. Epstein, E. M. Stolper, Geochim. Cosmochim. Acta **60**, 2635–2650 (1996).
17. J. P. Greenwood, S. Itoh, N. Sakamoto, E. P. Vicenzi, H. Yurimoto, Geophys. Res. Lett. **35**, L05203 (2008).
18. J. Farquar, M. H. Thiemens, J. Geophys. Res. **105**, (2000).
19. C. S. Romanek et al., Nature **372**, 655–657 (1994).
20. B. Jakosky, A. Zent, R. Zurek, Icarus **130**, 87–95 (1997).
21. H. R. Karlsson, R. N. Clayton, E. K. Gibson Jr., T. K. Mayeda, Science **255**, 1409–1411 (1992).
22. See the supplementary materials on Science Online.
23. L. A. Leshin et al., Lunar Planet. Sci. Conf., abstract 2220 (2013).
24. D. A. Fisher, Icarus **187**, 430–441 (2007) and references therein.
25. R. E. Novak et al., Bull. Am. Astron. Soc. **35**, 660 (2005).
26. T. Usui, C. Alexander, J. Wang, J. Simon, J. Jones, Earth Planet. Sci. Lett. **357-358**, 119–129 (2012).
27. H. Lammer et al., Space Sci. Rev. **174**, 113–154 (2013).
28. R. O. Pepin, Icarus **111**, 289–304 (1994).
29. L. Borg, M. J. Drake, J. Geophys. Res. **110**, E12S03 (2005).
30. P. B. Niles, L. A. Leshin, Y. Guan, Geochim. Cosmochim. Acta **69**, 2931–2944 (2005).
31. J. W. Valley et al., Science **275**, 1633–1638 (1997).
32. J. Farquhar, D. T. Johnston, Rev. Mineral. Geochem. **68**, 463–492 (2008).
33. B. M. Jakosky, J. H. Jones, Nature **370**, 328–329 (1994).
34. M. Grott, A. Morschhauser, D. Breuer, E. Hauber, EPSL **308**, 391–400 (2011).
35. J. P. Bibring et al., Science **312**, 400–404 (2006).
36. L. S. Rothman et al., J. Quant. Spectrosc. Radiat. Transf. **110**, 533–572 (2009).

Abundance and Isotopic Composition of Gases in the Martian Atmosphere from the Curiosity Rover

Paul R. Mahaffy,[1]* Christopher R. Webster,[2] Sushil K. Atreya,[3] Heather Franz,[1] Michael Wong,[3] Pamela G. Conrad,[1] Dan Harpold,[1] John J. Jones,[4] Laurie A. Leshin,[5] Heidi Manning,[6] Tobias Owen,[7] Robert O. Pepin,[8] Steven Squyres,[9] Melissa Trainer,[1] MSL Science Team†

Volume mixing and isotope ratios secured with repeated atmospheric measurements taken with the Sample Analysis at Mars instrument suite on the Curiosity rover are: carbon dioxide (CO_2), 0.960(±0.007); argon-40 (^{40}Ar), 0.0193(±0.0001); nitrogen (N_2), 0.0189(±0.0003); oxygen, 1.45(±0.09) × 10^{-3}; carbon monoxide, < 1.0 × 10^{-3}; and ^{40}Ar/^{36}Ar, 1.9(±0.3) × 10^3. The ^{40}Ar/N_2 ratio is 1.7 times greater and the ^{40}Ar/^{36}Ar ratio 1.6 times lower than values reported by the Viking Lander mass spectrometer in 1976, whereas other values are generally consistent with Viking and remote sensing observations. The ^{40}Ar/^{36}Ar ratio is consistent with martian meteoritic values, which provides additional strong support for a martian origin of these rocks. The isotopic signature δ^{13}C from CO_2 of ~45 per mil is independently measured with two instruments. This heavy isotope enrichment in carbon supports the hypothesis of substantial atmospheric loss.

The science and exploration goal of the Mars Science Laboratory (MSL) (1) is to advance our understanding of the potential of the present or past martian environments to support life. An understanding of how the present environment in Gale crater differs from the environment at the time of its forma-

tion requires comprehensive chemical characterization. The first set of experiments of the Sample Analysis at Mars (SAM) investigation (2) (Fig. 1) of the Curiosity rover included measurements of the chemical and isotopic composition of the atmosphere with sequences that employed two of SAM's three instruments. When

Supplementary Materials for

Isotope Ratios of H, C, and O in CO$_2$ and H$_2$O of the Martian Atmosphere

Chris R. Webster,* Paul R. Mahaffy, Gregory J. Flesch, Paul B. Niles, John H. Jones, Laurie A. Leshin, Sushil K. Atreya, Jennifer C. Stern, Lance E. Christensen, Tobias Owen, Heather Franz, Robert O. Pepin, Andrew Steele, the MSL Science Team

*Corresponding author. E-mail: Chris.R.Webster@jpl.nasa.gov

This PDF file includes:

Materials and Methods

<u>Spectral</u> <u>Data</u> <u>Processing</u>
      Spectral scan regions for TLS are shown in Fig. 1 and line parameters from HITRAN *(36)* are given in Tables S1 and S2 below. After normalization to the laser power and zero light pulse, spectral lines are processed individually by integrating over the line shape; line ratios are then related to those expected from calibration runs, using the HITRAN parameters if necessary to adjust for minor temperature differences. Details follow.

Theory
The Beer-Lambert law models the optical transmission of light through an absorbing medium:

$$I_v = I_0 e^{-k(v)\rho l}$$

where I_v is the transmitted light intensity at frequency v, I_0 is the incident light intensity, $k(v)$ is a line shaping function that may be Doppler, Lorenzian, or Voigt, although the Doppler lineshape is a close approximation at Mars atmospheric pressures. ρ is the number density and l is the path length in cm. We use this model to determine the abundances of individual absorption lines present in our sampled measurements and subsequently use those abundances to produce isotopic ratios. The model needs many input spectral parameters for temperature dependence, air broadening, ground state energy, etc., and we use the HITRAN database for this information *(36)*.

Normalization
For an amount of gas at a given pressure and temperature, the model will predict the depth and width (distribution in wave number) of the absorbing molecules in the gas sample for all sampled frequencies, allowing us to then compare our recorded spectra to the spectra produced by the model. But, in order to make this comparison, we must first normalize the recorded data. This entails:
1. Removing a "null pulse" which is a measurement of the background light taken with the laser off. We must be able to determine the direct absorption with respect to a percentage of transmitted light (i.e. 1% absorption: 99% transmission).
2. Removing any DC offsets in the harmonic spectra (described below).
3. Fit the baseline of the spectra. This sloping baseline results from the fact that the laser output power increases as it tunes through different wave numbers.
4. Assign a wave number (cm^{-1}) scale to the real spectra. We do this by using easily identifiable peaks of known wave number.

Once the spectra are normalized, we can then use the model to scale our real world data. Direct absorption spectra produce good results for gases that have line center absorption depths of 0.5% or greater. For greater resolution, we add a modulation to the laser current and then demodulate the returning detector signal at twice that frequency. This effectively gives us a second derivative of the direct spectra. Using this derivative or *2f* method, sensitivities of up to 2 parts in 10^5 are possible. See Webster et al. for a complete discussion *(37)*.

Producing Abundances

Using temperatures and pressures from our instrument for input, we iteratively run the model, varying the abundance in a converging algorithm until the synthetic spectra is the same size as our real spectra (within some determined threshold). The convergence criteria may be set to optimize for either the direct absorption or 2f spectra.

The algorithm is as follows (see Figs. S1 and S2):
1. Find the global max of the 2f absorption spectra (peak)
2. Find the two local minima (2f lobes)
3. Fit a line between the two lobes
4. Using the lobes as integration boundaries, find the area between the fitted line and the spectra for both the direct and 2f spectra. Ratio this area between real and synthetic spectra and if ratio is outside the convergence threshold, iterate with new abundance.

Once the measurements converge, we ratio the resulting areas of the real spectra to the synthetic spectra which has a known abundance. We do this for both the direct and harmonic spectra. In general, the direct spectra provide us with accuracy, since it is a very simple percentage measurement. The harmonic spectra, with its great sensitivity, provide greater precision for small changes in the signal, although determining the exact modulation values and gains introduce opportunity for error.

Although it is common practice to fit the entire spectra simultaneously, certain artifacts in our spectra make that approach problematic (see Instrument Issues section below). Instead, we process individual absorptions separately, which is not difficult at these Doppler-limited low pressures where the absorption lines tend to be clearly delineated. The benefits of this approach are 1) that we use the signal where it is strongest (between the 2f lobes), 2) it weakens the dependency on perfect baseline fitting, and 3) the boundaries of integration are set by the physics of absorption, rather than relying on a perfect wave number assignment.

Producing Isotope Ratios

Once we repeat this for every line of interest, we can create isotopic ratios for each data point (2 minute spectrum) according to the following standard isotope ratio formula for returning enrichment or depletion ratios in per mil. As an example, consider the case for comparing abundances of ^{13}C to ^{12}C in CO_2 to calculate $\delta^{13}C$ in units of per mil:

$$\left(\left[\frac{ {}^{13}CO2\_Observed / {}^{12}CO2\_Observed }{ {}^{13}CO2\_Standard / {}^{12}CO2\_Standard } \right] - 1 \right) * 1000$$

Instrument Issues

The HITRAN database reports its parameters to a few percent and we have refined some of those parameters through calibration testing. As for the artifacts mentioned above, several signal chain filters were set to values that attenuated the signal according to frequency, producing a "ring" on the direct absorption line shape. Fig. 2 in the main paper illustrates this effect, where part of the spectral region 1 is shown for CO_2 lines and is compared with the HITRAN calculations. Rather than try to remove the effects of that filter in our data, we build a software filter with identical behavior and make fine adjustments until our modeled output matches the line shape ring of our Mars spectra. In this way, we compare our Mars spectra with HITRAN-generated spectra that now have line shape rings included. Another potential issue is related to the susceptibility of the NIR laser to wavelength drift with heat sink temperature that depends on the Mars conditions (time of day). Across most of the scan range the laser tuning is constant and the effect is cancelled out. But we are watchful for situations where lines of interest are in the beginning of the scan where laser tuning rate is changing, and in these situations data is either discarded or the individual line results are given appropriately higher uncertainties.

<u>Calibration</u>

Calibration of the relative absorptions of isotopic pair lines was done pre-launch using either commercially-provided certified isotopic gas mixtures (Oztech) or specially prepared tanks (Cylinders A, B) whose isotopic content was determined by Isotope Ratio Mass Spectrometry (IRMS). For water isotopes, we used "Boulder water" independently certified by NOAA. See Table S3 for calibration gas isotopic values. Minor temperature and pressure interpolations are done using the HITRAN *(36)* line list. Although spectral SNR's are typically a few thousand, the data show scatter larger than this, and the reported results for any single run (Sol) are a mean value and either 1- or 2-standard errors from the mean (SEM) on the results (see Tables 1 and S4). Figure S3 shows our calibration plot of pre-launch and on-Mars cal gas results vs. retrieved measurements to show the excellent linearity over the measurement region.

Supplementary Text

<u>Isotope</u> <u>Ratio</u> <u>Results</u>

Tables of results on a sol-by-sol basis are given in Table S4. Because there is little water in the Martian atmosphere, the results for the δD values have quite high uncertainties compared to the result for the water evolved at lower temperatures from the Rocknest fines *(23)*.
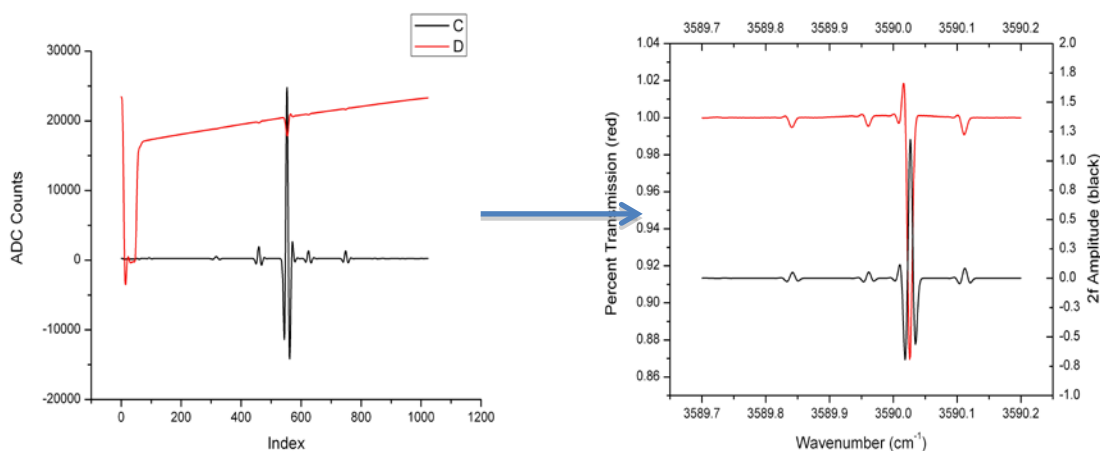
Fig. S1.

Example of normalization of real spectra for region 1. Lines can be identified from Fig. 1 in the main paper. The "C" or black traces are the second harmonic (2f) spectra, while the "D" or red traces are the direct absorption (DC) spectra.
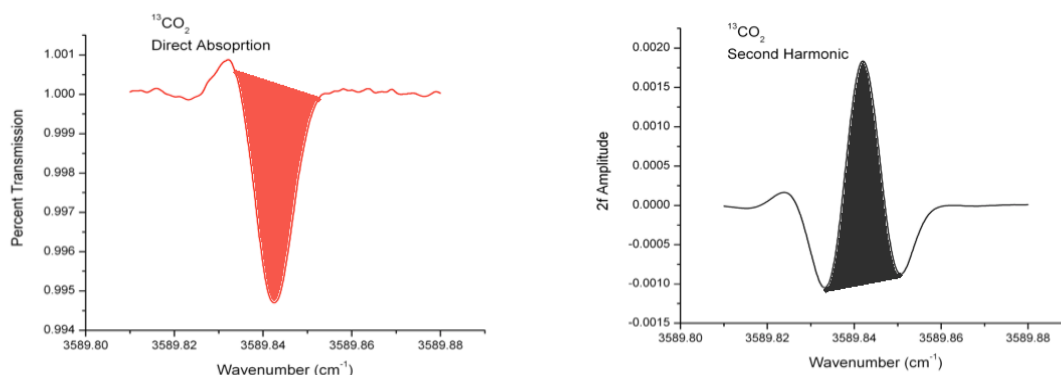
Fig. S2

Examples of direct (left) and 2f (right) line shapes for a single $^{13}CO_2$ line, showing the integrated area used in retrievals. This area is defined by the location of the two minima (lobes) in the 2f line shape mapped to the wave number scale in both line shapes.
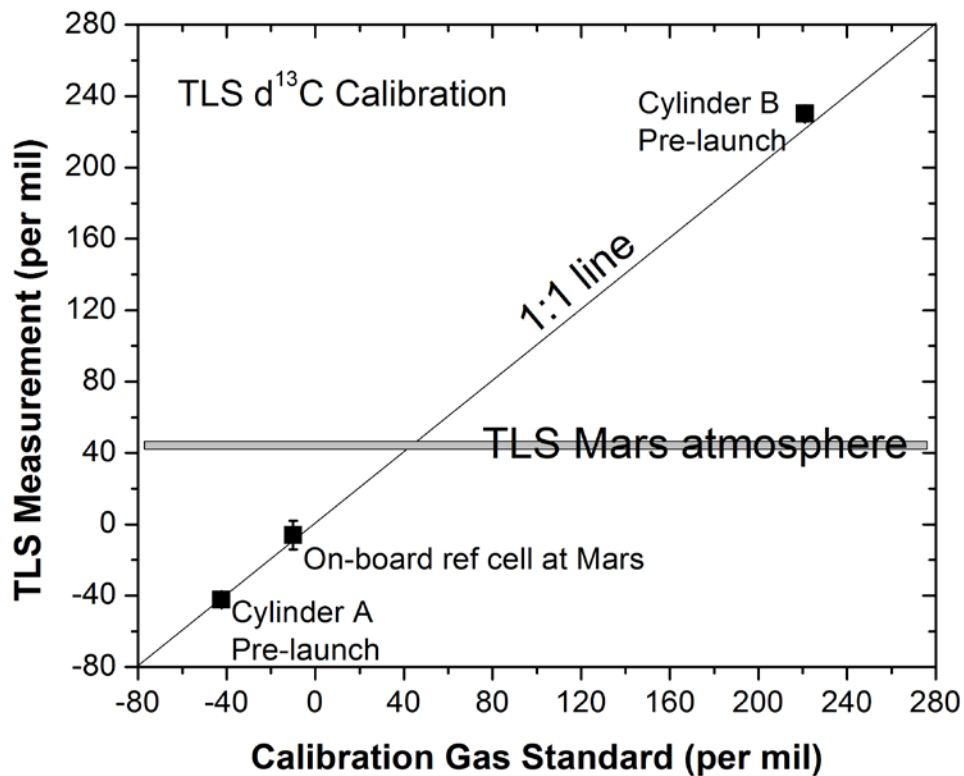
Fig. S3

Calibration plot showing pre-launch and on-Mars cal gas results vs. retrieved measurements to show excellent linearity over the measurement region.

Table S1.

HITRAN Line Parameters *(36)* for Spectral Region 1.

Line Designation	Isotopic Species	Wavenumber (cm^{-1})	Linestrength (cm^{-1}/ (molecule·cm^{-2}) at 296 K)	Ground State Energy (cm^{-1})
Z (H2O)	H_2O	3590.238310	1.222E-21	206.3014
X (H2O)	H_2O	3590.165390	5.164E-24	2251.8625
A (CO2)	CO_2	3590.116079	5.734E-23	1648.4209
Y (H2O)	HDO	3590.072290	4.478E-25	683.3240
B (CO2)	CO_2	3590.031510	1.341E-21	728.4124
C (CO2)	^{18}OCO	3589.966048	6.399E-23	319.8096
D (CO2)	$^{13}CO_2$	3589.846500	5.180E-23	843.0702
E (CO2)	^{17}OCO	3589.749440	3.057E-24	2.2717
F (H2O)	H_2O	3589.590960	4.599E-23	1437.9686

Table S2.

HITRAN Line Parameters *(36)* for Spectral Region 2.

Line Designation	Isotopic Species	Wavenumber (cm^{-1})	Linestrength (cm^{-1}/ (molecule·cm^{-2}) at 296 K)	Ground State Energy (cm^{-1})
Z (CO2)	^{18}OCO	3594.279835	3.294E-23	490.2111
Y (CO2)	CO_2	3594.216942	1.392E-21	801.1732
X (CO2)	$^{13}CO_2$	3594.160247	9.647E-23	704.3340
B (H2O)	$H_2^{18}O$	3594.061450	1.827E-23	78.9887
C (H2O)	H_2O	3593.974520	4.962E-22	756.7248
S (CO2)	$^{18}O^{13}CO$	3593.907244	9.883E-25	26.5089
W (CO2)	CO_2	3593.819208	3.554E-23	1805.2522
D (H2O)	H_2O	3593.791190	5.325E-24	382.5169
V (CO2)	^{18}OCO	3593.762005	3.640E-23	463.7240
E (H2O)	HDO	3593.597530	4.881E-24	513.2072
F (H2O)	$H_2^{18}O$	3593.545310	6.132E-24	133.4758
U (CO2)	^{17}OCO	3593.489040	4.590E-24	2.2717
T (CO2)	CO_2	3593.406043	1.411E-21	786.9028
G (H2O)	HDO	3593.317210	4.922E-24	512.5158
H (H2O)	H_2O	3593.197361	1.719E-02	602.7735

Table S3.

Calibration Standards Used in TLS as determined by Isotope Ratio Mass Spectrometry (IRMS).

Carbon Dioxide Isotope Values:		
Standard	$\delta^{13}C$	$\delta^{18}O$
Cylinder A	-43.02 ± 0.01	6.62 ± 0.01
Cylinder B	220.91 ± 0.05	476.05 ± 1.72
Cylinder C	475.64 ± 0.24	794.23 ± 9.9
Mars mix	-39.16 ± 0.05	0.61 ± 0.07
Oztech (ref cells)	-10.43 ± 0.05	31.24 ± 0.05
Water Isotope values:		
Standard	δD	$\delta^{18}O$
Boulder water	-110.11 ± 0.05	-14.91 ± 0.05

Table S4.

Sol by sol mean isotope ratio values (‰) and uncertainties (1_{SEM} ‰) measured by TLS. The first row for each entry is from Region 1, and the second row from Region 2. An "X" marks no reliable data retrieved due to SNR or other instrument issues. PTC = Possible Terrestrial Contamination; PC = Post-pyrolysis contamination.

Sol	$\delta^{13}C\_CO_2$	$\delta^{18}O\_CO_2$	$\delta^{17}O\_CO_2$	$\delta^{13}C^{18}O\_CO_2$	δD_H_2O
28	53.1 ± 5.7	41.5 ± 9.2	**X**	X	
	X	53.3 ± 2.8	22.7 ± 6.0	147 ± 12	PTC
53	45.3 ± 3.7	43.4 ± 5.3	30.6 ± 3.6	X	
	39.03 ± 5.7	36.48 ± 6.3	8.4 ± 7.6	X	PTC
73	34.3 ± 3.4	39.9 ± 7.5	28.5 ± 5.2	X	
	49.85 ± 4.0	38.3 ± 7.3	X	114 ± 27	$4,420 \pm 430$
79	41.1 ± 4.4	50.5 ± 4.0	32.1 ± 5.3	X	
	50.8 ± 11	63.2 ± 9.6	17.7 ± 15	112 ± 52	$5,480 \pm 980$
106	47.1 ± 1.9	61.6 ± 3.7	18.0 ± 2.9	X	PC
	50.1 ± 5.0	47.3 ± 4.0	10.2 ± 6.0	62 ± 18	
Range of values	34.3-53.1	36.5-63.2	8.4-32.1	62-147	4,420-5,480
Mean $\pm 1_{SEM}$	45.8 ± 2.1	47.6 ± 2.4	24.2 ± 2.0	109 ± 15.6	$4,950 \pm 540$
Mean $\pm 2_{SEM}$	**46 ± 4**	**48 ± 5**	**24 ± 5**	**109 ± 31**	**$4,950 \pm 1,080$**

Reference:

37. C. R. Webster, R. T. Menzies, and E. D. Hinkley, in *Laser Remote Chemical Analysis*, R. M. Measures, Ed. (Wiley, New York, New York) chap. 3, (1988).

MSL Science Team authors and affiliations:

Mars Science Laboratory Science Team	
Achilles, Cherie	Jacobs Technology (at NASA JSC)
Agard, Christophe	CNES (Centre National d'Etudes Spatiales)
Alves Verdasca, José Alexandre	CAB (Centro de Astrobiología)
Anderson, Robert	NASA JPL
Anderson, Ryan	USGS Flagstaff
Archer, Doug	NASA Postdoc Program (at NASA JSC)
Armiens-Aparicio, Carlos	CAB (Centro de Astrobiología)
Arvidson, Ray	WUSTL (Washington University in St. Louis)
Atlaskin, Evgeny	FMI (Finnish Meteorological Institute) and University of Helsinki
Aubrey, Andrew	NASA JPL
Baker, Burt	MSSS (Malin Space Science Systems)
Baker, Michael	Caltech
Balic-Zunic, Tonci	University of Copenhagen
Baratoux, David	IRAP (Institut de Recherche en Astrophysique et Planetologie)
Baroukh, Julien	CNES (Centre National d'Etudes Spatiales)
Barraclough, Bruce	PSI (Planetary Science Institute)
Bean, Keri	Texas A&M
Beegle, Luther	NASA JPL
Behar, Alberto	NASA JPL
Bell, James	ASU (Arizona State University)
Bender, Steve	PSI (Planetary Science Institute)
Benna, Mehdi	University of Maryland Baltimore County (at NASA GSFC)
Bentz, Jennifer	University of Saskatchewan
Berger, Gilles	IRAP (Institut de Recherche en Astrophysique et Planetologie)
Berger, Jeff	University of New Mexico (Western Univ. May 1)
Berman, Daniel	PSI (Planetary Science Institute)
Bish, David	Indiana University Bloomington
Blake, David F.	NASA Ames
Blanco Avalos, Juan J.	Universidad de Alcalá de Henares
Blaney, Diana	NASA JPL
Blank, Jen	BAER (at NASA Ames)
Blau, Hannah	University of Massachusetts
Bleacher, Lora	USRA-LPI (at NASA GSFC)
Boehm, Eckart	University of Kiel
Botta, Oliver	Swiss Space Office
Böttcher, Stephan	University of Kiel
Boucher, Thomas	University of Massachusetts
Bower, Hannah	University of Maryland College Park
Boyd, Nick	University of Guelph
Boynton, Bill	University of Arizona
Breves, Elly	Mount Holyoke College
Bridges, John	University of Leicester
Bridges, Nathan	APL (Johns Hopkins University Applied Physics Laboratory)
Brinckerhoff, William	NASA GSFC
Brinza, David	NASA JPL
Bristow, Thomas	NASA Postdoc Program (at NASA Ames)
Brunet, Claude	CSA (Canadian Space Agency)
Brunner, Anna	University of Maryland College Park (at GSFC)
Brunner, Will	inXitu
Buch, Arnaud	LGPM, Ecole Centrale Paris (Laboratoire Génie des Procédés et Matériaux)
Bullock, Mark	SwRI (Southwest Research Institute)
Burmeister, Sönke	University of Kiel
Cabane, Michel	LATMOS (Laboratoire Atmosphères, Milieux, Observations Spatiales)
Calef, Fred	NASA JPL
Cameron, James	Lightstorm Entertainment Inc.
Campbell, John "Iain"	University of Guelph
Cantor, Bruce	MSSS (Malin Space Science Systems)
Caplinger, Michael	MSSS (Malin Space Science Systems)
Caride Rodríguez, Javier	CAB (Centro de Astrobiología)
Carmosino, Marco	University of Massachusetts

Carrasco Blázquez, Isaías	CAB (Centro de Astrobiología)
Charpentier, Antoine	ATOS Origin
Chipera, Steve	Chesapeake Energy
Choi, David	NASA Postdoc Program (at NASA GSFC)
Clark, Benton	SSI (Space Science Institute)
Clegg, Sam	LANL (Los Alamos National Lab)
Cleghorn, Timothy	NASA JSC
Cloutis, Ed	University of Winnipeg
Cody, George	Carnegie Institution of Washington
Coll, Patrice	LISA (Laboratoire Interuniversitaire des Systèmes Atmosphériques), Université Paris
Conrad, Pamela	NASA GSFC
Coscia, David	LATMOS (Laboratoire Atmosphères, Milieux, Observations Spatiales)
Cousin, Agnès	LANL (Los Alamos National Lab)
Cremers, David	ARA (Applied Research Associates, Inc.)
Crisp, Joy	NASA JPL
Cros, Alain	IRAP (Institut de Recherche en Astrophysique et Planetologie)
Cucinotta, Frank	NASA JSC
d'Uston, Claude	IRAP (Institut de Recherche en Astrophysique et Planetologie)
Davis, Scott	MSSS (Malin Space Science Systems)
Day, Mackenzie "Kenzie"	University of Texas at Austin
de la Torre Juarez, Manuel	NASA JPL
DeFlores, Lauren	NASA JPL
DeLapp, Dorothea	LANL (Los Alamos National Lab)
DeMarines, Julia	Denver Museum of Nature & Science
DesMarais, David	NASA Ames
Dietrich, William	University of California Berkeley
Dingler, Robert	LANL (Los Alamos National Lab)
Donny, Christophe	CNES (Centre National d'Etudes Spatiales)
Downs, Bob	University of Arizona
Drake, Darrell	retired
Dromart, Gilles	LGL-TPE (Laboratoire de Géologié de Lyon : Terre, Planète, Environnement)
Dupont, Audrey	CS Systemes d'Information
Duston, Brian	MSSS (Malin Space Science Systems)
Dworkin, Jason	NASA GSFC
Dyar, M. Darby	Mount Holyoke College
Edgar, Lauren	ASU (Arizona State University)
Edgett, Kenneth	MSSS (Malin Space Science Systems)
Edwards, Christopher	Caltech
Edwards, Laurence	NASA Ames
Ehlmann, Bethany	Caltech
Ehresmann, Bent	SwRI (Southwest Research Institute)
Eigenbrode, Jen	NASA GSFC
Elliott, Beverley	University of New Brunswick
Elliott, Harvey	University of Michigan Ann Arbor
Ewing, Ryan	University of Alabama
Fabre, Cécile	G2R (Géologié et Gestion des Ressources Minérales et Energétique)
Fairén, Alberto	Cornell University
Farley, Ken	Caltech
Farmer, Jack	ASU (Arizona State University)
Fassett, Caleb	Mount Holyoke College
Favot, Laurent	Capgemini France
Fay, Donald	MSSS (Malin Space Science Systems)
Fedosov, Fedor	Space Research Institute
Feldman, Jason	NASA JPL
Feldman, Sabrina	NASA JPL
Fisk, Marty	Oregon State University
Fitzgibbon, Mike	University of Arizona

Floyd, Melissa	NASA GSFC
Flückiger, Lorenzo	Carnegie Mellon University (at NASA Ames)
Forni, Olivier	IRAP (Institut de Recherche en Astrophysique et Planetologie)
Fraeman, Abby	WUSTL (Washington University in St. Louis)
Francis, Raymond	University of Western Ontario
François, Pascaline	LISA (Laboratoire Interuniversitaire des Systèmes Atmosphériques), Université Paris
Freissinet, Caroline	NASA Postdoc Program (at NASA GSFC)
French, Katherine Louise	MIT
Frydenvang, Jens	University of Copenhagen
Gaboriaud, Alain	CNES (Centre National d'Etudes Spatiales)
Gailhanou, Marc	CNRS (Centre National de la Recherche Scientifique)
Garvin, James	NASA GSFC
Gasnault, Olivier	IRAP (Institut de Recherche en Astrophysique et Planetologie)
Geffroy, Claude	IC2MP (Institut de Chimie des Milieux et Matériaux de Poitiers)
Gellert, Ralf	University of Guelph
Genzer, Maria	FMI (Finnish Meteorological Institute)
Glavin, Daniel	NASA GSFC
Godber, Austin	ASU (Arizona State University)
Goesmann, Fred	Max Planck Institute for Solar System Research
Goetz, Walter	Max Planck Institute for Solar System Research
Golovin, Dmitry	Space Research Institute
Gómez Gómez, Felipe	Centro de Astrobiología
Gómez-Elvira, Javier	Centro de Astrobiología
Gondet, Brigitte	IAS (Institut d'Astrophysique Spatiale)
Gordon, Suzanne	University of New Mexico
Gorevan, Stephen	Honeybee Robotics
Grant, John	Smithsonian Institution
Griffes, Jennifer	Caltech
Grinspoon, David	Denver Museum of Nature & Science
Grotzinger, John	Caltech
Guillemot, Philippe	CNES (Centre National d'Etudes Spatiales)
Guo, Jingnan	SwRI (Southwest Research Institute)
Gupta, Sanjeev	Imperial College
Guzewich, Scott	NASA Postdoc Program (at NASA GSFC)
Haberle, Robert	NASA Ames
Halleaux, Douglas	University of Michigan Ann Arbor
Hallet, Bernard	University of Washington Seattle
Hamilton, Vicky	(SwRI) Southwest Research Institute
Hardgrove, Craig	MSSS (Malin Space Science Systems)
Harker, David	MSSS (Malin Space Science Systems)
Harpold, Daniel	NASA GSFC
Harri, Ari-Matti	FMI (Finnish Meteorological Institute)
Harshman, Karl	University of Arizona
Hassler, Donald	SwRI (Southwest Research Institute)
Haukka, Harri	FMI (Finnish Meteorological Institute)
Hayes, Alex	Cornell University
Herkenhoff, Ken	USGS Flagstaff
Herrera, Paul	MSSS (Malin Space Science Systems)
Hettrich, Sebastian	CAB (Centro de Astrobiología)
Heydari, Ezat	Jackson State University
Hipkin, Victoria	CSA (Canadian Space Agency)
Hoehler, Tori	NASA Ames
Hollingsworth, Jeff	NASA Ames
Hudgins, Judy	Salish Kootenai College
Huntress, Wesley	Retired
Hurowitz, Joel	NASA JPL
Hviid, Stubbe	Max Planck Institute for Solar System Research
Iagnemma, Karl	MIT

Indyk, Steve	Honeybee Robotics
Israël, Guy	CNRS and LATMOS
Jackson, Ryan	LANL (Los Alamos National Lab)
Jacob, Samantha	University of Hawai'i at Manoa
Jakosky, Bruce	University of Colorado Boulder
Jensen, Elsa	MSSS (Malin Space Science Systems)
Jensen, Jaqueline Kløvgaard	University of Copenhagen
Johnson, Jeffrey	APL (Johns Hopkins University Applied Physics Laboratory)
Johnson, Micah	Microtel (at NASA GSFC)
Johnstone, Steve	LANL (Los Alamos National Lab)
Jones, Andrea	USRA-LPI (at NASA GSFC)
Joseph, Jonathan	Cornell University
Jun, Insoo	NASA JPL
Kah, Linda	University of Tennessee Knoxville
Kahanpää, Henrik	FMI (Finnish Meteorological Institute)
Kahre, Melinda	NASA Ames
Karpushkina, Natalya	Space Research Institute
Kasprzak, Wayne	NASA GSFC
Kauhanen, Janne	FMI (Finnish Meteorological Institute)
Keely, Leslie	NASA Ames
Kemppinen, Osku	FMI (Finnish Meteorological Institute)
Keymeulen, Didier	NASA JPL
Kim, Myung-Hee	USRA (at NASA JSC)
Kinch, Kjartan	University of Copenhagen
King, Penny	ANU (Australian National University)
Kirkland, Laurel	LPI (Lunar and Planetary Institute)
Kocurek, Gary	University of Texas at Austin
Koefoed, Asmus	University of Copenhagen
Köhler, Jan	University of Kiel
Kortmann, Onno	University of California Berkeley
Kozyrev, Alexander	Space Research Institute
Krezoski, Jill	MSSS (Malin Space Science Systems)
Krysak, Daniel	MSSS (Malin Space Science Systems)
Kuzmin, Ruslan	Space Research Institute and Vernadsky Institute
Lacour, Jean Luc	CEA (Commissariat à l'Énergie Atomique et aux Énergies Alternatives)
Lafaille, Vivian	CNES (Centre National d'Etudes Spatiales)
Langevin, Yves	IAS (Institut d'Astrophysique Spatiale)
Lanza, Nina	LANL (Los Alamos National Lab)
Lasue, Jeremie	IRAP (Institut de Recherche en Astrophysique et Planetologie)
Le Mouélic, Stéphane	LPGN (Laboratoire de Planétologie et Géodynamique de Nantes)
Lee, Ella Mae	USGS Flagstaff
Lee, Qiu-Mei	IRAP (Institut de Recherche en Astrophysique et Planetologie)
Lees, David	Carnegie Mellon University (at NASA Ames)
Lefavor, Matthew	Microtel (at NASA GSFC)
Lemmon, Mark	Texas A&M
Lepinette Malvitte, Alain	CAB (Centro de Astrobiología)
Léveillé, Richard	CSA (Canadian Space Agency)
Lewin-Carpintier, Éric	ISTerre (Institut des Sciences de la Terre)
Lewis, Kevin	Princeton University
Li, Shuai	Brown University
Lipkaman, Leslie	MSSS (Malin Space Science Systems)
Little, Cynthia	LANL (Los Alamos National Lab)
Litvak, Maxim	Space Research Institute
Lorigny, Eric	CNES (Centre National d'Etudes Spatiales)
Lugmair, Guenter	UCSD (University of California San Diego)
Lundberg, Angela	Delaware State University
Lyness, Eric	Microtel (at NASA GSFC)
Madsen, Morten	University of Copenhagen

Maki, Justin	NASA JPL
Malakhov, Alexey	Space Research Institute
Malespin, Charles	USRA (at NASA GSFC)
Malin, Michael	MSSS (Malin Space Science Systems)
Mangold, Nicolas	LPGN (Laboratoire de Planétologie et Géodynamique de Nantes)
Manhes, Gérard	Retired
Manning, Heidi	Concordia College
Marchand, Geneviève	CSA (Canadian Space Agency)
Marín Jiménez, Mercedes	CAB (Centro de Astrobiología)
Martín García, César	University of Kiel
Martin, Dave	NASA GSFC
Martin, Mildred	Catholic University of America (at NASA GSFC)
Martínez-Frías, Jesús	Centro de Astrobiología
Martín-Soler, Javier	CAB (Centro de Astrobiología)
Martín-Torres, F. Javier	Centro de Astrobiología
Mauchien, Patrick	CEA (Commissariat à l'Énergie Atomique et aux Énergies Alternatives)
Maurice, Sylvestre	IRAP (Institut de Recherche en Astrophysique et Planetologie)
McAdam, Amy	NASA GSFC
McCartney, Elaina	MSSS (Malin Space Science Systems)
McConnochie, Timothy	University of Maryland (at NASA GSFC)
McCullough, Emily	University of Western Ontario
McEwan, Ian	Ashima Research
McKay, Christopher	NASA Ames
McLennan, Scott	SUNY Stony Brook
McNair, Sean	MSSS (Malin Space Science Systems)
Melikechi, Noureddine	Delaware State University
Meslin, Pierre-Yves	IRAP (Institut de Recherche en Astrophysique et Planetologie)
Meyer, Michael	NASA Headquarters
Mezzacappa, Alissa	Delaware State University
Miller, Hayden	Caltech
Miller, Kristen	MIT
Milliken, Ralph	Brown University
Ming, Douglas	NASA JSC
Minitti, Michelle	ASU (Arizona State University)
Mischna, Michael	NASA JPL
Mitrofanov, Igor	Space Research Institute
Moersch, Jeff	University of Tennessee Knoxville
Mokrousov, Maxim	Space Research Institute
Molina Jurado, Antonio	CAB (Centro de Astrobiología)
Moores, John	York University
Mora-Sotomayor, Luis	CAB (Centro de Astrobiología)
Morookian, John Michael	NASA JPL
Morris, Richard	NASA JSC
Morrison, Shaunna	University of Arizona
Mueller-Mellin, Reinhold	University of Kiel
Muller, Jan-Peter	UCL (University College London)
Muñoz Caro, Guillermo	CAB (Centro de Astrobiología)
Nachon, Marion	LPGN (Laboratoire de Planétologie et Géodynamique de Nantes)
Navarro López, Sara	CAB (Centro de Astrobiología)
Navarro-González, Rafael	UNAM (University Nacional Autónoma de México)
Nealson, Kenneth	USC (University of Southern California)
Nefian, Ara	Carnegie Mellon University (at NASA Ames)
Nelson, Tony	LANL (Los Alamos National Lab)
Newcombe, Megan	Caltech
Newman, Claire	Ashima Research
Newsom, Horton	University of New Mexico
Nikiforov, Sergey	Space Research Institute
Nixon, Brian	MSSS (Malin Space Science Systems)

Noe Dobrea, Eldar	PSI (Planetary Science Institute)
Nolan, Thomas	Nolan Engineering (at NASA GSFC)
Oehler, Dorothy	Jacobs Technology (at NASA JSC)
Ollila, Ann	University of New Mexico
Olson, Timothy	Salish Kootenai College
Pablo Hernández, Miguel Ángel de	Universidad de Alcalá de Henares
Paillet, Alexis	CNES (Centre National d'Etudes Spatiales)
Pallier, Etienne	IRAP (Institut de Recherche en Astrophysique et Planetologie)
Palucis, Marisa	University of California Berkeley
Parker, Timothy	NASA JPL
Parot, Yann	IRAP (Institut de Recherche en Astrophysique et Planetologie)
Patel, Kiran	Global Science & Technology, Inc. (at NASA GSFC)
Paton, Mark	FMI (Finnish Meteorological Institute)
Paulsen, Gale	Honeybee Robotics
Pavlov, Alex	NASA GSFC
Pavri, Betina	NASA JPL
Peinado-González, Verónica	CAB (Centro de Astrobiología)
Peret, Laurent	ATOS Origin
Perez, Rene	CNES (Centre National d'Etudes Spatiales)
Perrett, Glynis	University of Guelph
Peterson, Joe	SwRI (Southwest Research Institute)
Pilorget, Cedric	Caltech
Pinet, Patrick	IRAP (Institut de Recherche en Astrophysique et Planetologie)
Pla-García, Jorge	CAB (Centro de Astrobiología)
Plante, Ianik	USRA (at NASA JSC)
Poitrasson, Franck	CNRS (Centre National de la Recherche Scientifique) and GET (Géosciences Environnement Toulouse)
Polkko, Jouni	FMI (Finnish Meteorological Institute)
Popa, Radu	USC (University of Southern California)
Posiolova, Liliya	MSSS (Malin Space Science Systems)
Posner, Arik	NASA Headquarters
Pradler, Irina	University of Guelph
Prats, Benito	eINFORMe Inc. (at NASA GSFC)
Prokhorov, Vasily	Space Research Institute
Purdy, Sharon Wilson	Smithsonian Institution
Raaen, Eric	NASA GSFC
Radziemski, Leon	Piezo Energy Technologies, Tucson
Rafkin, Scot	SwRI (Southwest Research Institute)
Ramos, Miguel	Universidad de Alcalá de Henares
Rampe, Elizabeth	NASA Postdoc Program (at NASA JSC)
Raulin, François	LISA (Laboratoire Interuniversitaire des Systèmes Atmosphériques), Université Paris
Ravine, Michael	MSSS (Malin Space Science Systems)
Reitz, Günther	DLR (Deutsches Zentrum für Luft- und Raumfahrt)
Rennó, Nilton	University of Michigan Ann Arbor
Rice, Melissa	NASA Postdoc Program (at Caltech)
Richardson, Mark	Ashima Research
Robert, François	(LMCM) Laboratoire de Minéralogie et Cosmochimie du Muséum
Robertson, Kevin	Brown University
Rodriguez Manfredi, José Antonio	CAB (Centro de Astrobiología)
Romeral-Planelló, Julio J.	CAB (Centro de Astrobiología)
Rowland, Scott	University of Hawai'i at Manoa
Rubin, David	USGS Santa Cruz
Saccoccio, Muriel	CNES (Centre National d'Etudes Spatiales)
Salamon, Andrew	MSSS (Malin Space Science Systems)
Sandoval, Jennifer	MSSS (Malin Space Science Systems)
Sanin, Anton	Space Research Institute
Sans Fuentes, Sara Alejandra	CAB (Centro de Astrobiología)
Saper, Lee	MSSS (Malin Space Science Systems)
Sarrazin, Philippe	inXitu

Sautter, Violaine	LMCM (Laboratoire de Minéralogie et Cosmochimie du Muséum)
Savijärvi, Hannu	University of Helsinki
Schieber, Juergen	Indiana University Bloomington
Schmidt, Mariek	Brock University
Schmidt, Walter	FMI (Finnish Meteorological Institute)
Scholes, Daniel "Dan"	WUSTL (Washington University in St. Louis)
Schoppers, Marcel	NASA JPL
Schröder, Susanne	IRAP (Institut de Recherche en Astrophysique et Planetologie)
Schwenzer, Susanne	Open University
Sebastian Martinez, Eduardo	CAB (Centro de Astrobiología)
Sengstacken, Aaron	NASA JPL
Shterts, Ruslan	Space Research Institute
Siebach, Kirsten	Caltech
Siili, Tero	FMI (Finnish Meteorological Institute)
Simmonds, Jeff	NASA JPL
Sirven, Jean-Baptiste	CEA (Commissariat à l'Énergie Atomique et aux Énergies Alternatives)
Slavney, Susie	WUSTL (Washington University in St. Louis)
Sletten, Ronald	University of Washington Seattle
Smith, Michael	NASA GSFC
Sobrón Sánchez, Pablo	CSA (Canadian Space Agency)
Spanovich, Nicole	NASA JPL
Spray, John	University of New Brunswick
Squyres, Steven	Cornell University
Stack, Katie	Caltech
Stalport, Fabien	LISA (Laboratoire Interuniversitaire des Systèmes Atmosphériques)
Stein, Thomas	WUSTL (Washington University in St. Louis)
Stewart, Noel	Salish Kootenai College
Stipp, Susan Louise Svane	University of Copenhagen
Stoiber, Kevin	MSSS (Malin Space Science Systems)
Stolper, Ed	Caltech
Sucharski, Bob	USGS Flagstaff
Sullivan, Rob	Cornell University
Summons, Roger	MIT
Sumner, Dawn	University of California Davis
Sun, Vivian	Brown University
Supulver, Kimberley	MSSS (Malin Space Science Systems)
Sutter, Brad	Jacobs Technology (at NASA JSC)
Szopa, Cyril	LATMOS (Laboratoire Atmosphères, Milieux, Observations Spatiales)
Tan, Florence	NASA GSFC
Tate, Christopher	University of Tennessee Knoxville
Teinturier, Samuel	LATMOS (Laboratoire Atmosphères, Milieux, Observations Spatiales)
ten Kate, Inge	Utrecht University
Thomas, Peter	Cornell University
Thompson, Lucy	University of New Brunswick
Tokar, Robert	Planetary Science Institute
Toplis, Mike	IRAP (Institut de Recherche en Astrophysique et Planetologie)
Torres Redondo, Josefina	CAB (Centro de Astrobiología)
Trainer, Melissa	NASA GSFC
Treiman, Allan	(LPI) Lunar and Planetary Institute
Tretyakov, Vladislav	Space Research Institute
Urqui-O'Callaghan, Roser	CAB (Centro de Astrobiología)
Van Beek, Jason	MSSS (Malin Space Science Systems)
Van Beek, Tessa	MSSS (Malin Space Science Systems)
VanBommel, Scott	University of Guelph
Vaniman, David	PSI (Planetary Science Institute)
Varenikov, Alexey	Space Research Institute
Vasavada, Ashwin	NASA JPL
Vasconcelos, Paulo	University of Queensland

Vicenzi, Edward	Smithsonian Institution
Vostrukhin, Andrey	Space Research Institute
Voytek, Mary	NASA Headquarters
Wadhwa, Meenakshi	ASU (Arizona State University)
Ward, Jennifer	WUSTL (Washington University in St. Louis)
Weigle, Eddie	Big Head Endian LLC
Wellington, Danika	ASU (Arizona State University)
Westall, Frances	CNRS (Centre National de la Recherche Scientifique)
Wiens, Roger Craig	LANL (Los Alamos National Lab)
Wilhelm, Mary Beth	NASA Ames and Georgia Institute of Technology
Williams, Amy	University of California Davis
Williams, Joshua	University of New Mexico
Williams, Rebecca	PSI (Planetary Science Institute)
Williams, Richard B. "Mouser"	LANL (Los Alamos National Lab)
Wilson, Mike	UCSF (University of California San Francisco) (at NASA Ames)
Wimmer-Schweingruber, Robert	University of Kiel
Wolff, Mike	SSI (Space Science Institute)
Wong, Mike	University of Michigan Ann Arbor
Wray, James	MSSS (Malin Space Science Systems)
Wu, Megan	MSSS (Malin Space Science Systems)
Yana, Charles	CNES (Centre National d'Etudes Spatiales)
Yen, Albert	NASA JPL
Yingst, Aileen	PSI (Planetary Science Institute) (at University of Wisconsin)
Zeitlin, Cary	SwRI (Southwest Research Institute)
Zimdar, Robert	MSSS (Malin Space Science Systems)
Zorzano Mier, María-Paz	CAB (Centro de Astrobiología)

References and Notes

1. P. R. Mahaffy, C. R. Webster, M. Cabane, P. G. Conrad, P. Coll, S. K. Atreya, R. Arvey, M. Barciniak, M. Benna, L. Bleacher, W. B. Brinckerhoff, J. L. Eigenbrode, D. Carignan, M. Cascia, R. A. Chalmers, J. P. Dworkin, T. Errigo, P. Everson, H. Franz, R. Farley, S. Feng, G. Frazier, C. Freissinet, D. P. Glavin, D. N. Harpold, D. Hawk, V. Holmes, C. S. Johnson, A. Jones, P. Jordan, J. Kellogg, J. Lewis, E. Lyness, C. A. Malespin, D. K. Martin, J. Maurer, A. C. McAdam, D. McLennan, T. J. Nolan, M. Noriega, A. A. Pavlov, B. Prats, E. Raaen, O. Sheinman, D. Sheppard, J. Smith, J. C. Stern, F. Tan, M. Trainer, D. W. Ming, R. V. Morris, J. Jones, C. Gundersen, A. Steele, J. Wray, O. Botta, L. A. Leshin, T. Owen, S. Battel, B. M. Jakosky, H. Manning, S. Squyres, R. Navarro-González, C. P. McKay, F. Raulin, R. Sternberg, A. Buch, P. Sorensen, R. Kline-Schoder, D. Coscia, C. Szopa, S. Teinturier, C. Baffes, J. Feldman, G. Flesch, S. Forouhar, R. Garcia, D. Keymeulen, S. Woodward, B. P. Block, K. Arnett, R. Miller, C. Edmonson, S. Gorevan, E. Mumm, The Sample Analysis at Mars investigation and instrument suite. *Space Sci. Rev.* **170**, 401–478 (2012). doi:10.1007/s11214-012-9879-z

2. J. P. Grotzinger, J. Crisp, A. R. Vasavada, R. C. Anderson, C. J. Baker, R. Barry, D. F. Blake, P. Conrad, K. S. Edgett, B. Ferdowski, R. Gellert, J. B. Gilbert, M. Golombek, J. Gómez-Elvira, D. M. Hassler, L. Jandura, M. Litvak, P. Mahaffy, J. Maki, M. Meyer, M. C. Malin, I. Mitrofanov, J. J. Simmonds, D. Vaniman, R. V. Welch, R. C. Wiens; Mars Science Laboratory Mission and Science Investigation, Mars Science Laboratory mission and science investigation. *Space Sci. Rev.* **170**, 5–56 (2012). doi:10.1007/s11214-012-9892-2

3. P. R. Mahaffy *et al*., Abundance and isotopic composition of gases in the Martian atmosphere: First results from the Mars Curiosity Rover. *Science* **341**, 263–266 (2013).

4. C. R. Webster, P. R. Mahaffy, S. K. Atreya, G. J. Flesch, K. A. Farley, Measurements of Mars methane at Gale Crater by the Curiosity Rover. *Lunar Planet. Sci. Conf*., abstract 1366 (2013).

5. B. M. Jakosky, R. J. Phillips, Mars' volatile and climate history. *Nature* **412**, 237–244 (2001). doi:10.1038/35084184 Medline

6. M. B. McElroy, Y. L. Yung, A. O. Nier, Isotopic composition of nitrogen: Implications for the past history of Mars' atmosphere. *Science* **194**, 70–72 (1976). doi:10.1126/science.194.4260.70 Medline

7. T. Owen, J.-P. Maillard, C. de Bergh, B. L. Lutz, Deuterium on Mars: The abundance of HDO and the value of D/H. *Science* **240**, 1767–1770 (1988). doi:10.1126/science.240.4860.1767 Medline

8. R. H. Carr, M. M. Grady, I. P. Wright, C. T. Pillinger, Martian atmospheric carbon-dioxide and weathering products in SNC meteorites. *Nature* **314**, 248–250 (1985). doi:10.1038/314248a0

9. V. A. Krasnopolsky, J. P. Maillard, T. C. Owen, R. A. Toth, M. D. Smith, Oxygen and carbon isotope ratios in the Martian atmosphere. *Icarus* **192**, 396–403 (2007). doi:10.1016/j.icarus.2007.08.013

10. P. B. Niles, D. C. Catling, G. Berger, E. Chassefière, B. L. Ehlmann, J. R. Michalski, R. Morris, S. W. Ruff, B. Sutter, Geochemistry of carbonates on Mars: Implications for climate history and nature of aqueous environments. *Space Sci. Rev.* **174**, 301–328 (2013). doi:10.1007/s11214-012-9940-y

11. A. O. Nier, M. B. McElroy, Structure of the neutral upper atmosphere of Mars: Results from Viking 1 and Viking 2. *Science* **194**, 1298–1300 (1976). doi:10.1126/science.194.4271.1298 Medline

12. P. B. Niles, W. V. Boynton, J. H. Hoffman, D. W. Ming, D. Hamara, Stable isotope measurements of martian atmospheric CO_2 at the Phoenix landing site. *Science* **329**, 1334–1337 (2010). doi:10.1126/science.1192863 Medline

13. R. E. Criss, *Principles of Stable Isotope Composition* (Oxford Univ. Press, Oxford, 1999).

14. C. R. Webster, A. J. Heymsfield, Water isotope ratios D/H, $^{18}O/^{16}O$, $^{17}O/^{16}O$ in and out of clouds map dehydration pathways. *Science* **302**, 1742–1745 (2003). doi:10.1126/science.1089496 Medline

15. P. Hartogh, D. C. Lis, D. Bockelée-Morvan, M. de Val-Borro, N. Biver, M. Küppers, M. Emprechtinger, E. A. Bergin, J. Crovisier, M. Rengel, R. Moreno, S. Szutowicz, G. A. Blake, Ocean-like water in the Jupiter-family comet 103P/Hartley 2. *Nature* **478**, 218–220 (2011). doi:10.1038/nature10519 Medline

16. L. A. Leshin, S. Epstein, E. M. Stolper, Hydrogen isotope geochemistry of SNC meteorites. *Geochim. Cosmochim. Acta* **60**, 2635–2650 (1996). doi:10.1016/0016-7037(96)00122-6

17. J. P. Greenwood, S. Itoh, N. Sakamoto, E. P. Vicenzi, H. Yurimoto, Hydrogen isotope evidence for loss of water from Mars through time. *Geophys. Res. Lett.* **35**, L05203 (2008). doi:10.1029/2007GL032721

18. J. Farquar, M. H. Thiemens, Oxygen cycle of the Martian atmosphere-regolith system: $\delta^{17}O$ of secondary phases in Nakhla and Lafayette. *J. Geophys. Res.* **105**, (2000). 10.1029/1999JE001194

19. C. S. Romanek, M. M. Grady, I. P. Wright, D. W. Mittlefehldt, R. A. Socki, C. T. Pillinger, E. K. Gibson Jr., Record of fluid-rock interactions on Mars from the meteorite ALH84001. *Nature* **372**, 655–657 (1994). doi:10.1038/372655a0 Medline

20. B. Jakosky, A. Zent, R. Zurek, The Mars water cycle: Determining the role of exchange with the regolith. *Icarus* **130**, 87–95 (1997). doi:10.1006/icar.1997.5799

21. H. R. Karlsson, R. N. Clayton, E. K. Gibson Jr., T. K. Mayeda, Water in SNC meteorites: Evidence for a martian hydrosphere. *Science* **255**, 1409–1411 (1992). doi:10.1126/science.11537889 Medline

22. See the supplementary materials on *Science* Online.

23. L. A. Leshin *et al.*, Integrated results from analysis of the Rocknest aeolian deposit by the Curiosity Rover. *Lunar Planet. Sci. Conf.*, abstract 2220 (2013).

24. D. A. Fisher, Mars water isotope D/H history in the strata of the North Polar Cap: Inferences about the water cycle. *Icarus* **187**, 430–441 (2007) and references therein. doi:10.1016/j.icarus.2006.10.032

25. R. E. Novak, M. J. Mumma, S. Lee, L. Ivanov, B. Bonev, G. Villanueva, Mapping of D/H and ozone in the martian atmosphere near perihelion. *Bull. Am. Astron. Soc.* **35**, 660 (2005).

26. T. Usui, C. Alexander, J. Wang, J. Simon, J. Jones, Origin of water and mantle-crust interactions on Mars inferred from hydrogen isotopes and volatile element abundances of olivine-hosted melt inclusions of primitive shergottites. *Earth Planet. Sci. Lett.* **357-358**, 119–129 (2012). doi:10.1016/j.epsl.2012.09.008

27. H. Lammer, E. Chassefière, Ö. Karatekin, A. Morschhauser, P. B. Niles, O. Mousis, P. Odert, U. V. Möstl, D. Breuer, V. Dehant, M. Grott, H. Gröller, E. Hauber, L. B. S. Pham, Outgassing history and escape of the martian atmosphere and water inventory. *Space Sci. Rev.* **174**, 113–154 (2013). doi:10.1007/s11214-012-9943-8

28. R. O. Pepin, Evolution of the martian atmosphere. *Icarus* **111**, 289–304 (1994). doi:10.1006/icar.1994.1146

29. L. Borg, M. J. Drake, A review of meteorite evidence for the timing of magmatism and of surface or near-surface liquid water on Mars. *J. Geophys. Res.* **110**, E12S03 (2005). doi:10.1029/2005JE002402

30. P. B. Niles, L. A. Leshin, Y. Guan, Microscale carbon isotope variability in ALH84001 carbonates and a discussion of possible formation environments. *Geochim. Cosmochim. Acta* **69**, 2931–2944 (2005). doi:10.1016/j.gca.2004.12.012

31. J. W. Valley, J. M. Eiler, C. M. Graham, E. K. Gibson, C. S. Romanek, E. M. Stolper, Low-temperature carbonate concretions in the Martian meteorite ALH84001: Evidence from stable isotopes and mineralogy. *Science* **275**, 1633–1638 (1997). doi:10.1126/science.275.5306.1633 Medline

32. J. Farquhar, D. T. Johnston, The oxygen cycle of the terrestrial planets: Insights into the processing and history of oxygen in surface environments. *Rev. Mineral. Geochem.* **68**, 463–492 (2008). doi:10.2138/rmg.2008.68.16

33. B. M. Jakosky, J. H. Jones, Evolution of water on Mars. *Nature* **370**, 328–329 (1994). doi:10.1038/370328a0

34. M. Grott, A. Morschhauser, D. Breuer, E. Hauber, Volcanic outgassing of CO_2 and H_2O on Mars. *EPSL* **308**, 391–400 (2011). doi:10.1016/j.epsl.2011.06.014

35. J. P. Bibring, Y. Langevin, J. F. Mustard, F. Poulet, R. Arvidson, A. Gendrin, B. Gondet, N. Mangold, P. Pinet, F. Forget, M. Berthé, J. P. Bibring, A. Gendrin, C. Gomez, B. Gondet, D. Jouglet, F. Poulet, A. Soufflot, M. Vincendon, M. Combes, P. Drossart, T. Encrenaz, T. Fouchet, R. Merchiorri, G. Belluci, F. Altieri, V. Formisano, F. Capaccioni, P. Cerroni, A. Coradini, S. Fonti, O. Korablev, V. Kottsov, N. Ignatiev, V. Moroz, D. Titov, L. Zasova, D. Loiseau, N. Mangold, P. Pinet, S. Douté, B. Schmitt, C. Sotin, E. Hauber, H. Hoffmann, R. Jaumann, U. Keller, R. Arvidson, J. F. Mustard, T. Duxbury, F. Forget, G. Neukum, Global mineralogical and aqueous Mars history derived from OMEGA/Mars Express data. *Science* **312**, 400–404 (2006). doi:10.1126/science.1122659 Medline

36. L. S. Rothman, I. E. Gordon, A. Barbe, D. C. Benner, P. F. Bernath, M. Birk, V. Boudon, L. R. Brown, A. Campargue, J.-P. Champion, K. Chance, L. H. Coudert, V. Dana, V. M. Devi, S. Fally, J.-M. Flaud, R. R. Gamache, A. Goldman, D. Jacquemart, I. Kleiner, N.

Lacome, W. J. Lafferty, J.-Y. Mandin, S. T. Massie, S. N. Mikhailenko, C. E. Miller, N. Moazzen-Ahmadi, O. V. Naumenko, A. V. Nikitin, J. Orphal, V. I. Perevalov, A. Perrin, A. Predoi-Cross, C. P. Rinsland, M. Rotger, M. Šimečková, M. A. H. Smith, K. Sung, S. A. Tashkun, J. Tennyson, R. A. Toth, A. C. Vandaele, J. Vander Auwera, The HITRAN 2008 molecular spectroscopic database. *J. Quant. Spectrosc. Radiat. Transf.* **110**, 533–572 (2009). doi:10.1016/j.jqsrt.2009.02.013

37. C. R. Webster, R. T. Menzies, E. D. Hinkley, in *Laser Remote Chemical Analysis*, R. M. Measures, Ed. (Wiley, New York, 1988), chap. 3.